ELSEVIER

Neurobiology of Disease

www.elsevier.com/locate/ynbdi
Neurobiology of Disease 28 (2007) 184–196

Abnormal glutamate homeostasis and impaired synaptic plasticity and learning in a mouse model of tuberous sclerosis complex

Ling-Hui Zeng,[a,1] Yannan Ouyang,[a,1,2] Vered Gazit,[a,1] John R. Cirrito,[a] Laura A. Jansen,[a,3] Kevin C. Ess,[a,4] Kelvin A. Yamada,[a,b] David F. Wozniak,[b,c] David M. Holtzman,[a,b] David H. Gutmann,[a] and Michael Wong[a,b,*]

[a]*Department of Neurology, Washington University School of Medicine, St. Louis, MO 63110, USA*
[b]*The Hope Center for Neurological Disorders, Washington University School of Medicine, St. Louis, MO 63110, USA*
[c]*Department of Psychiatry, Washington University School of Medicine, St. Louis, MO 63110, USA*

Received 7 May 2007; revised 30 June 2007; accepted 4 July 2007
Available online 21 July 2007

Mice with inactivation of the Tuberous sclerosis complex-1 (*Tsc1*) gene in glia (*Tsc1*^{GFAP}CKO mice) have deficient astrocyte glutamate transporters and develop seizures, suggesting that abnormal glutamate homeostasis contributes to neurological abnormalities in these mice. We examined the hypothesis that *Tsc1*^{GFAP}CKO mice have elevated extracellular brain glutamate levels that may cause neuronal death, abnormal glutamatergic synaptic function, and associated impairments in behavioral learning. *In vivo* microdialysis documented elevated glutamate levels in hippocampi of *Tsc1*^{GFAP}CKO mice and several cell death assays demonstrated neuronal death in hippocampus and neocortex. Impairment of long-term potentiation (LTP) with tetanic stimulation was observed in hippocampal slices from *Tsc1*^{GFAP}CKO mice and was reversed by low concentrations of NMDA antagonist, indicating that excessive synaptic glutamate directly inhibited LTP. Finally, *Tsc1*^{GFAP}CKO mice exhibited deficits in two hippocampal-dependent learning paradigms. These results suggest that abnormal glutamate homeostasis predisposes to excitotoxic cell death, impaired synaptic plasticity and learning deficits in *Tsc1*^{GFAP}CKO mice.

Keywords: Glia; Astrocyte; Glutamate transporter; Microdialysis; Long-term potentiation; Learning; Excitotoxicity; Seizure; Epilepsy

Introduction

Tuberous sclerosis complex (TSC) is a relatively common multi-system genetic disease caused by mutation of either the *TSC1* or *TSC2* gene (Crino et al., 2006; Kwiatkowski, 2003; Sparagana and Roach, 2000). Neurological symptoms are usually the most disabling clinical problems associated with TSC and typically include seizures, autism, mental retardation, and learning disabilities. Current treatments of the neurological manifestations of TSC are purely symptom-based and are largely ineffective. Thus, understanding the pathophysiology of TSC is critical for developing novel, more effective therapies for the neurological symptoms in TSC. The neuropathological hallmark of brains from TSC patients are areas of disrupted cortical lamination, termed tubers, which likely represent the epileptogenic foci for seizures and also contribute to the cognitive deficits in TSC (Doherty et al., 2005; Goodman et al., 1997). Cortical tubers demonstrate dramatic histopathological abnormalities in glia, suggesting that defective glial function may be centrally involved in the pathogenesis of TSC (Gutmann et al., 2000; Ess et al., 2004). In this regard, we have previously demonstrated that conditional *Tsc1* gene inactivation primarily in glia of mice (*Tsc1*^{GFAP}CKO mice) results in progressive epilepsy, encephalopathy, and premature death (Uhlmann et al., 2002). However, the specific mechanisms causing neuronal dysfunction in *Tsc1*^{GFAP}CKO mice are unknown.

Glutamate, the major excitatory neurotransmitter in mammalian brain, may have detrimental effects on neurons when present in excessive amounts and has been implicated in the pathogenesis of a number of neurological disorders. Impairment of glutamate uptake by astrocytes can lead to excessive extracellular glutamate levels, resulting in abnormal synaptic function under some conditions (Mennerick and Zorumski, 1994; Tong and Jahr, 1994), impaired long-term potentiation (Katagiri et al., 2001), and excitotoxic neuronal death (Rothstein et al., 1996; Tanaka et al., 1997), which may all cause cognitive dysfunction. Furthermore, inactivation of

* Corresponding author. Department of Neurology, Box 8111, Washington University School of Medicine, 660 South Euclid Avenue, St. Louis, MO 63110, USA. Fax: +1 314 362 9462.
E-mail address: wong_m@wustl.edu (M. Wong).
[1] These authors contributed equally to this paper.
[2] Present address: Saban Research Institute, Children's Hospital Los Angeles, Los Angeles, CA 90027, USA.
[3] Present address: Department of Neurology, Division of Pediatric Neurology, University of Washington and Children's Hospital and Regional Medical Center, Seattle, WA 98105, USA.
[4] Present address: Department of Neurology, Vanderbilt University, Nashville, TN 37232, USA.
Available online on ScienceDirect (www.sciencedirect.com).

0969-9961/$ - see front matter © 2007 Elsevier Inc. All rights reserved.
doi:10.1016/j.nbd.2007.07.015

the astrocyte glutamate transporters, GLT-1 or GLAST, results in decreased seizure threshold or spontaneous seizures in mice (Tanaka et al., 1997; Watanabe et al., 1999). We have previously shown that astrocytes from *Tsc1*^{GFAP}CKO mice exhibit decreased expression and function of GLT-1 and GLAST (Wong et al., 2003), suggesting the possibility that abnormal glutamate homeostasis could also contribute to neuronal dysfunction in the *Tsc1*^{GFAP}CKO mice. Thus, in the present study, we examined the hypothesis that *Tsc1*^{GFAP}CKO mice have elevated extracellular glutamate levels, which may contribute to excitotoxic neuronal death, abnormal glutamatergic synaptic physiology, and impaired behavioral conditioning and learning.

Materials and methods

Animals

Tsc1$^{flox/flox}$-GFAP-Cre (*Tsc1*^{GFAP}CKO) knockout mice with conditional inactivation of the *Tsc1* gene in glia were produced using Cre-Lox technology as described previously (Uhlmann et al., 2002). *Tsc1*$^{flox/+}$-GFAP-Cre or *Tsc1*$^{flox/flox}$ littermates were used as controls in these experiments and have previously been found to have no abnormal phenotype (Uhlmann et al., 2002). Care and use of animals conformed to a protocol approved by the Washington University School of Medicine Animal Studies Committee.

In vivo microdialysis

Four-week-old mice were implanted with microdialysis probes as previously described (Cirrito et al., 2003, 2005). Briefly, under isoflurane anesthesia, guide cannulae (BR-style, Bioanalytical Systems, Indianapolis, IN) were inserted stereotaxically into the left hippocampus (bregma −3.1 mm, 2.5 mm lateral to midline, and 0.6 mm below dura at a 12° angle). After the guide cannulae were cemented, 2-mm microdialysis probes (BR-2, 38 kDa MWCO membrane, Bioanalytical Systems) were inserted through the guides into the hippocampus. Mice were allowed to recover from anesthesia and were housed in a Raturn Cage system (Bioanalytical Systems), which permitted freedom of movement and ad libitum food and water for the remainder of the experiment. The microdialysis probe was connected to a Univentor syring pump (SciPro) and artificial cerebrospinal fluid [ACSF (in mM): 1.3 $CaCl_2$, 1.2 $MgSO_4$, 3 KCl, 0.4 KH_2PO_4, 25 $NaHCO_3$, and 122 NaCl, pH 7.35] was perfused through the microdialysis probe. All dialysate samples were collected with a refrigerated fraction collector into polypropylene tubes for subsequent measurement of glutamate concentration, as described below. To ensure that brain extracellular fluid (ECF) glutamate levels reached a steady-state concentration after probe insertion, six 1-h samples were taken at a constant flow rate during an initial equilibration phase prior to starting the protocol below. After a stable baseline was obtained, an extrapolated zero flow protocol was used to calculate the *in vivo* concentration of glutamate within the brain ECF (Menacherry et al., 1992; Cirrito et al., 2003), by measuring glutamate concentrations from dialysate samples acquired at different flow rates and extrapolating back to zero flow rate, at which point the dialysate should reach equilibrium with and equal the *in vivo* ECF glutamate concentration. The extrapolation was based on a second-order polynomial fit: $y = a*x^2 + b*x + E$, where y = glutamate concentration, x = flow rate, and E = extrapolated *in vivo* ECF concentration at zero flow rate. To assess whether the microdialysis sampling technique and other biological factors were consistent between different conditions (e.g., control vs. *Tsc1*^{GFAP}CKO mice), the percentage recovery of glutamate at each flow rate was determined and compared by the following equation: $(C_x/E)*100$, where C_x is the measured glutamate concentration at a given flow rate and E is the *in vivo* concentration calculated by extrapolation. At the end of microdialysis, animals were anesthetized with isobutyl and transcardially perfused with phosphate-buffered saline (PBS) followed by 4% paraformaldehyde in PBS pH 7.4 to allow histological confirmation of the microdialysis probe location in the hippocampus.

Glutamate concentration assay

Dialysate glutamate concentrations were measured using an Amplex red glutamic acid/glutamate oxidase assay kit (Molecular Probes, Eugene, OR) on the same day microdialysis was performed. For each sample, a total volume of 100 µl per microplate well was obtained by mixing 50 µl of sample with 50 µl of working solution (100 µM Amplex Red, 0.25 U/ml horseradish peroxidase (HRP), 0.08 U/ml L-glutamate oxidase, 0.5 U/ml L-glutamate-pyruvate transaminase, and 200 µM L-alanine). Samples were then incubated at 37 °C for 30 min and analyzed with a FL600 microplate reader (BioTek, Winooski, VT) with 530 nm excitation and 590 nm emission wavelengths. Glutamate concentrations of samples were determined by interpolation from a standard curve derived by measurements of other samples with known, pre-measured concentrations of glutamate. Each point was corrected for background fluorescence by subtracting values derived from glutamate-free control samples.

Cell death assays

1- and 3-month-old control or *Tsc1*^{GFAP}CKO mice were anesthetized with ketamine and perfused transcardially with 0.1 M phosphate-buffered saline (PBS), pH 7.4, followed by 4% paraformaldehyde in 0.1 M PBS. Brains were removed immediately after perfusion and placed in 4% paraformaldehyde for 30 min at 4 °C and then stored in 0.1 M PBS containing 30% sucrose for 72 h at 4 °C. 50 µm coronal sections were cut with a vibratome and kept in cryoprotective solution (ethylene glycol and sucrose in 0.1 M PBS, pH 7.4) at −20 °C until used for immunostaining or TUNEL studies.

The TUNEL assay was performed on brain sections by standard protocol using the ApopTag-Fluorescein Kit (Serologicals Corporation, Norcross, GA). Briefly, sections were washed with 0.1 M PBS and pretreated sequentially with 0.3% Triton X for 15 min at room temperature (RT), 20 µg/ml proteinase K for 20 min at 37 °C, and 0.2% H_2O_2 for 20 min at RT, with intervening washes in 0.1 M PBS. Tissue was then placed in the equilibration buffer for 1 min at room temperature, followed by incubation in the reaction buffer containing terminal deoxynucleotidyltransferase enzyme (TdT) for 1 h at 37 °C. The reaction was then terminated by transferring sections to stop buffer for 10 min at RT and sections were washed in PBS three times for 5 min each. The sections were then incubated with FITC-conjugated anti-digoxigenin antibody for 30 min at RT, rinsed in PBS, and mounted in Vectashield with DAPI (Vector Laboratories, Burlingame, CA). Negative controls for each TUNEL experiment omitted the TdT enzyme from the reaction mixture. Positive controls for the TUNEL procedure were utilized from the kit.

Immunostaining to caspase-3 was performed by standard techniques using a rabbit polyclonal caspase-3 antibody (Cell Signaling Technologies, Beverly, MA) and Alexa Fluor 488 anti-rabbit secondary antibody (Molecular Probes, Eugene, OR). Labeling for Fluoro-Jade B (Chemicon International, Temecula, CA) was performed using previously published methods (Schmued and Hopkins, 2000). To identify neurons positive for TUNEL, double labeling was performed with a mouse monoclonal anti-NeuN antibody (Chemicon International). Neocortex and hippocampus of fixed coronal sections were examined for positively stained neurons using confocal microscopy. For quantification, the number of positive neurons per section were counted in frontal sections (~1.5–2.5 mm posterior to bregma) containing neocortex and hippocampus by an observer blinded to the genotype of the sections.

Slice electrophysiology

Horizontal entorhinal cortex–hippocampal slices (400 μm) were prepared with a vibratome from 2- to 4-week-old control or *Tsc1*^{GFAP}CKO mice, using standard methods as described previously (Wong et al., 2003). Slices were placed in a submerged recording chamber and perfused continuously with an ACSF containing (in mM): 124 NaCl, 3 KCl, 2.5 $CaCl_2$, 1.3 $MgCl_2$, 1.3 NaH_2PO_4, 22 $NaHCO_3$, and 10 glucose. Patch pipettes were filled with (in mM): 130 CsCl, 4 NaCl, 0.5 $CaCl_2$, 10 HEPES, 5 EGTA, and 2 $MgCl_2$. QX-314 (10 mM) was also added to the pipette solution to block sodium currents. Pyramidal neurons in the CA1 region were directly visualized on an upright microscope with differential interference contrast/infrared optics. Whole cell voltage clamp recordings were obtained and analyzed using an Axopatch 200B amplifier, Digidata 1322 data acquisition system, and pCLAMP 8 software (Molecular Devices, Sunnyvale, CA). Series resistance compensation of 70–85% was used. Membrane capacitance was calculated from fitting of current transient responses to small hyperpolarizing voltage steps. Excitatory postsynaptic currents were activated at a holding potential of −60 mV by electrical stimulation of Schaffer collaterals in stratum radiatum with a tungsten concentric bipolar stimulating electrode (0.1 ms, 0.1 Hz). The amplitude of the stimulation pulses was adjusted to the lowest intensity necessary to induce a maximal response (0.5–2 mA). Five current traces per condition were averaged and analyzed with pCLAMP software. The decay phase of synaptic currents was fitted by a two-component exponential Chebyshev method. All single cell experiments were performed at both room temperature (~25 °C) and at ~33 °C. For studies of non-NMDA currents, MK-801 (10 μM) and bicuculline (25 μM) were added to the ACSF. For isolation of NMDA currents, magnesium was omitted and CNQX (20 μM), bicuculline (25 μM) and glycine (10 μM) were added to the ACSF. GABAergic inhibitory postsynaptic currents were isolated by addition of MK-801 (10 μM) and CNQX (20 μM) to the standard ACSF. All drugs were purchased from Sigma (St. Louis, MO), unless otherwise specified.

Other experiments examining extracellular field EPSPs and long-term potentiation were performed in coronal (400 μm) hippocampal slices from ~8-week-old control and *Tsc1*^{GFAP}CKO mice. Extracellular field potentials were recorded with glass microelectrodes filled with ACSF from the stratum radiatum of CA1 region. Signals were recorded by an Axoclamp 2B amplifier in bridge mode with additional amplification from a Warner Instrument DC amplifier and saved and analyzed by pCLAMP software. Stable, baseline field EPSPs of approximately one-third of maximal amplitude were activated by stimulation of the Schaffer collateral pathway with a bipolar stimulating electrode at 0.016 Hz. To induce LTP, a series of 4 tetani of 100 Hz stimuli for 1 s were applied with each tetanus separated by 30 s.

Behavioral studies

Sensorimotor battery

During the early postweaning period (P24 ± 1 day), *Tsc1*^{GFAP}CKO (n = 10) mice and littermate controls (n = 9) were evaluated on a battery of tests (walking initiation, inclined and inverted screens, platform, ledge, and pole) designed to assess balance, strength, and coordination as previously described (Wozniak et al., 2004). Two trials were administered and averaged for each test with a 2-h interval intervening between trials.

1-h locomotor activity

Locomotor activity was quantified using a computerized, photobeam system (MotorMonitor, Hamilton-Kinder, LLC, Poway, CA) according to previously published methods (Wozniak et al., 2004). The mice were tested in transparent polystyrene enclosures (47.6 cm × 25.4 cm × 20.6 cm high) just before beginning spatial (place) learning trials in the water maze (see below) on P30 (±1 day). The dependent variables analyzed included the number of ambulations (whole body movements), rearings, distance traveled in the periphery, distance traveled in the central area of the "field", and time spent and entries made into the center during a 1-h test period. Analysis of measures involving behaviors emitted in the center was used to evaluate possible alterations in emotionality beyond changes in activity.

Morris water navigation

Spatial learning and memory capabilities were assessed during the early juvenile period using the Morris water navigation test utilizing procedures similar to previously published methods (Wozniak et al., 2004). The protocol included conducting cued (visible platform), place (submerged and not visible platform), and probe (platform removed) trials in a round pool (118 cm inner diameter) of opaque water. Swim paths were tracked and recorded by a computerized system (Polytrack, San Diego Instruments, San Diego, CA), which calculated escape path length and latency. Swimming speeds were also calculated for cued and place trials. Mice were first trained on the cued condition (P28 ± 1 day) to determine if non-associative factors (e.g., sensorimotor or visual disturbances or alterations in motivation) were likely to affect acquisition performance during subsequent place trials. Mice received 4 trials per day for 2 consecutive days of cued training, using an intertrial interval of approximately 20 min, and allowing the mouse to remain on the platform for 15 s. The platform was moved to a different location for each trial within a day in the presence of very few distal cues thus substantially limiting spatial learning during this time. Three days after completing the cued trials, the mice were trained on the "place" condition to learn the location of a submerged (hidden) platform. The place trials were conducted in the presence of several salient distal cues positioned around the room to facilitate association of the spatial cues with the submerged platform location. During place training, the mice

were given 4 trials per day for 5 days (60 s maximum for a trial) with the platform remaining in the same location for all place trials. The daily protocol involved administering 2 blocks of 2 consecutive trials with each block being separated by approximately 1 h and a mouse being released from a different quadrant for each trial. A probe trial was administered approximately 1 h after completion of the place trials on the 5th day of place trials to evaluate retention of the platform location. During the 60-s probe trial, the escape platform was removed and a mouse was placed in the quadrant diagonally opposite from the previous platform location. Times spent in the pool quadrants, and the number of crossings made over the previous platform location (platform crossings), were recorded.

Conditioned fear (contextual and auditory cue tests)

2 or 3 days after completing water maze testing, the mice were evaluated on the conditioned fear test (P39±1 day) using a protocol similar to our previously published methods (Khuchua et al., 2003) except that in the present study, freezing behavior was scored by a computerized video-based image analysis system (see below). Briefly, the mice were trained and tested in two Plexiglas conditioning chambers (26 cm×18 cm×18 cm high) (Med-Associates, St. Albans, VT) with each chamber differing in terms of visual, tactile, and olfactory cues present. On Day 1, each mouse was placed into the conditioning chamber for 5 min. Freezing behavior was quantified during a 2-min baseline period, after which an 80 dB tone (conditioned stimulus; CS) consisting of broadband white noise was presented for 20 s. During the last second of the pulse, the mice received a 1.0 mA continuous foot shock (unconditioned stimulus; US). This CS–US (tone–shock) pairing was repeated each minute over the next 2 min, and freezing was quantified after each of the three tone–shock pairings. The mice were removed from the testing chamber 40 s after the third shock and returned to their home cages. 24 h later, each mouse was placed in the same conditioning chamber in which it was trained to test contextual fear, which involved quantifying freezing behavior for 8 min. 24 h later, each mouse was placed into a different chamber (with different cues present) to be evaluated on the auditory cue test. The mice were observed for 10 min in this "altered context" and freezing behavior was quantified during a 2-min baseline period and over a subsequent 8-min period, during which time the auditory cue (tone; CS) was presented. Freezing was quantified using FreezeFrame image analysis software (Actimetrics, Evanston, IL) which allowed for simultaneous visualization of behavior while adjusting a "freezing threshold" which categorized behavior as freezing or not freezing during 0.75-s intervals. Freezing was defined as no movement except for that associated with normal respiration and the data was presented as percent of time spent freezing.

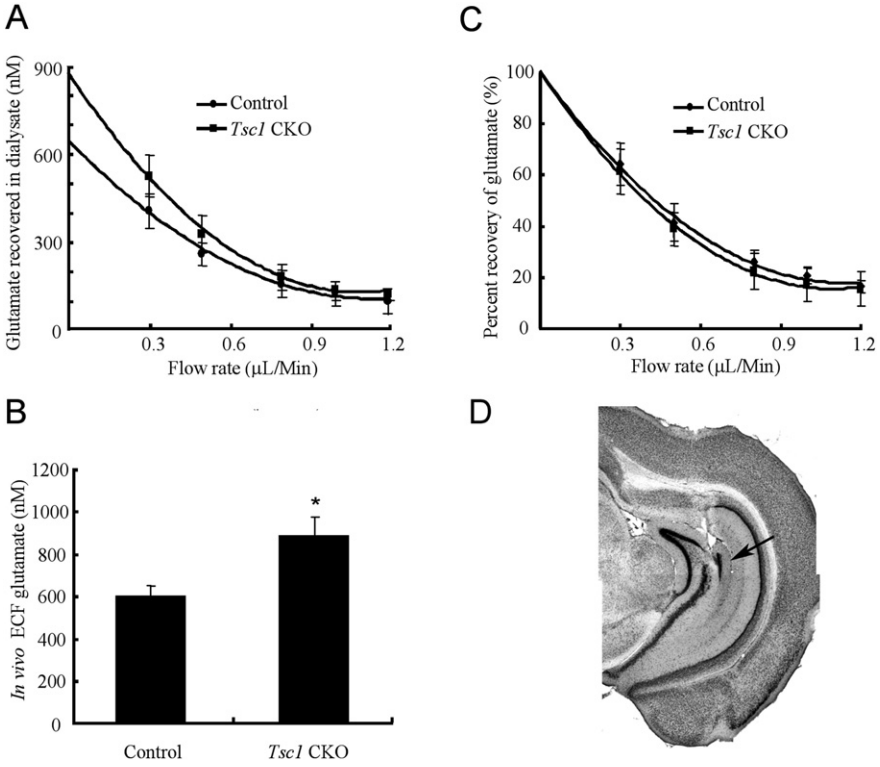

Fig. 1. Extracellular glutamate is elevated in the hippocampus of *Tsc1*^{GFAP}CKO mice *in vivo*. (A) Extracellular glutamate concentrations were measured from control and *Tsc1*^{GFAP}CKO mice with microdialysis at different flow rates. Fitted polynomial curves show the dependence of the measured dialysate glutamate concentration on flow rate for each group and allow extrapolation of the absolute ECF glutamate concentration by the extrapolated zero flow method (see Materials and methods). (B) Average *in vivo* ECF glutamate concentration of control and *Tsc1*^{GFAP}CKO mice was determined based on the extrapolated ECF glutamate concentration calculated individually for each mouse. *Tsc1*^{GFAP}CKO mice had significantly elevated ECF glutamate concentrations compared to controls ($n=6$ mice per group; *$p<0.05$). (C) Recovery percentage of glutamate at various flow rates was not significantly different between control and KO mice, indicating that the microdialysis technique and other biological factors were consistent between the two groups. (D) Representative microdialysis probe site in the hippocampus of 4-week-old mice.

After completing the conditioned fear testing, the mice were evaluated for their shock sensitivity to determine if fear conditioning may have been affected by this variable. The levels of shock that were necessary to elicit flinching, running, vocalizing, or jumping were determined for each mouse using our previously published procedures (Khuchua et al., 2003). The shock sensitivity measures and all other behavioral tests were conducted by observers who were unaware of the genotypic status of individual mice. In addition, mice were carefully monitored for seizure-like behaviors, and those that exhibited such behaviors were not tested on any behavioral measure until they appeared to be fully recovered.

Statistics

For behavioral experiments, analysis of variance (ANOVA) models with repeated measures (including Huynh–Feldt adjustment) were used. The model typically contained one between-subjects variable (genotype) and one within-subjects variable (e.g., blocks of trials) and included Bonferroni corrections for multiple comparisons. For other experiments, two-tailed *t*-tests were used for all comparisons of quantitative data between two groups (e.g., control and *Tsc1*^{GFAP}CKO mice). One-way ANOVA was used in the hippocampal slice LTP experiments, comparing three groups (e.g., control, *Tsc1*^{GFAP}CKO, *Tsc1*^{GFAP}CKO + APV). All numerical data are presented as mean ± standard error of the mean (SEM). Statistical significance was defined as $p < 0.05$.

Results

Extracellular glutamate is elevated in the hippocampus of Tsc1^{GFAP}*CKO mice in vivo*

Our previous work has demonstrated a >75% decrease in GLT-1 and GLAST expression and a corresponding decrease in astrocyte glutamate transporter functional activity in the hippocampus of *Tsc1*^{GFAP}CKO mice (Wong et al., 2003). Given this impairment in astrocyte glutamate transport in *Tsc1*^{GFAP}CKO mice, we performed *in vivo* microdialysis to determine the ECF concentration of glutamate in the hippocampus in 4-week-old *Tsc1*^{GFAP}CKO and control mice. The 4-week age was chosen as a time that should precede seizure onset (Uhlmann et al., 2002; Erbayat-Altay et al., 2007). Within 3 h of microdialysis probe insertion, glutamate levels achieved a steady-state in both control and *Tsc1*^{GFAP}CKO mice (data not shown), and between 4 and 6 h following probe insertion, the relative dialysate glutamate concentration was significantly higher in *Tsc1*^{GFAP}CKO mice (131.9 ± 15.4 nM vs. 84.2 ± 12.2 nM in controls; $n = 5$ mice per group, $p < 0.05$). To calculate the absolute ECF glutamate concentration *in vivo*, an extrapolated zero flow protocol was then utilized, in which glutamate concentrations were measured at different flow rates and extrapolation was performed to a theoretical zero flow rate (Fig. 1A), at which point the dialysate and ECF should reach equilibrium and equal the *in vivo* ECF glutamate concentration (Menacherry et al., 1992). Using this

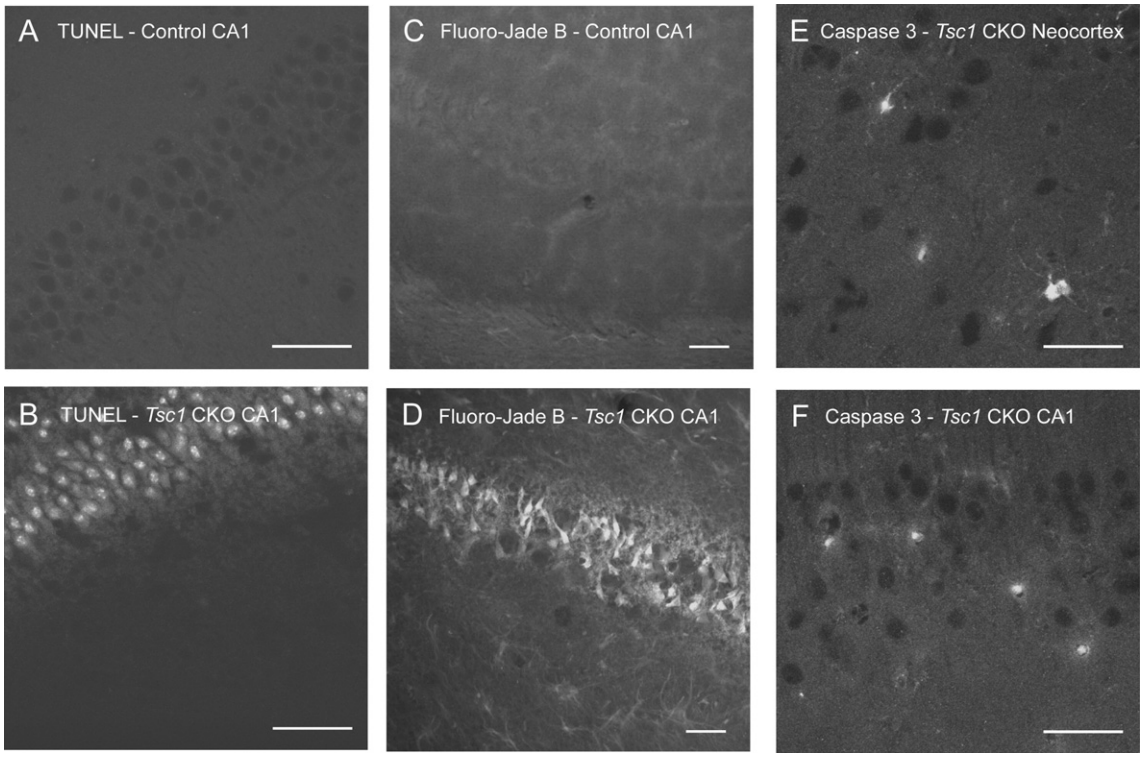

Fig. 2. Neuronal death occurs in the neocortex and hippocampus of *Tsc1*^{GFAP}CKO mice. (A, B) Representative examples of TUNEL-positive cells in the CA1 region of hippocampus (B) of a 3-month-old *Tsc1*^{GFAP}CKO mouse, compared to absent TUNEL staining in a 3-month-old control mouse (A). (C, D) Representative examples of Fluoro-Jade B-positive cells in CA1 region of hippocampus (D) in the same *Tsc1*^{GFAP}CKO mouse as in *B*, compared to absent Fluoro-Jade B staining in a 3-month-old control mouse (C). (E, F) Representative examples of caspase-3 staining in neocortex (E) and hippocampus (F) in a 1-month-old *Tsc1*^{GFAP}CKO mouse. Calibration bars = 50 μm for all panels.

method individually in each mouse, the average ECF glutamate concentration was significantly elevated in *Tsc1*^{GFAP}CKO mice (Fig. 1B; 902.1±88.1 nM vs. 607.3±52.1 for controls; $p<0.01$, $n=6$ mice per group). By comparison, the percentage recovery of glutamate (determined by dividing the measured glutamate concentration at a given flow rate by the absolute extrapolated concentration) was not different between *Tsc1*^{GFAP}CKO mice and wild type mice at each flow rate (Fig. 1C), indicating that the microdialysis technique and other potentially confounding biological factors were consistent between the two groups. Evidence of histological damage from the microdialysis technique was minimal (Fig. 1D; see also Cirrito et al., 2003).

Neuronal death occurs in Tsc1^{GFAP}CKO mice independent of seizures

Since increased extracellular glutamate may result in neuronal excitotoxicity, we examined neuronal death in control and *Tsc1*^{GFAP}CKO mice at 1 and 3 months of age using multiple methods, including TUNEL, caspase-3, and Fluoro-Jade B labeling. The 1- and 3-month time points were chosen to represent times before and after onset of seizures, based on previous video-EEG studies (Uhlmann et al., 2002; Erbayat-Altay et al., 2007; see Discussion), thus controlling for the additional effects of seizures on neuronal death. TUNEL-positive immunoreactivity was detected in the neocortex, hippocampal CA1 and CA3 pyramidal cell layers, and dentate gyrus (granular and subgranular layers) in both 1- and 3-month-old *Tsc1*^{GFAP}CKO mice (Figs. 2B, 3A, and 4). By comparison, no TUNEL-positive cells were seen in control mice (Fig. 2A), with the exception of a few cells in the subgranular layer of dentate gyrus (DG), consistent with previous reports and corresponding to a region of ongoing neurogenesis (Biebl et al., 2000). Although there was a trend toward increased TUNEL-positive cells in the hippocampus (but not neocortex) of *Tsc1*^{GFAP}CKO mice at 3 months compared to 1 month, this increase was not statistically significant (Fig. 3A). Fluoro-Jade B (Fig. 2D) and caspase-3 (Figs. 2E, F and 3B) staining revealed similar spatial and temporal patterns of positive cells.

The pattern of TUNEL, caspase-3, and Fluoro-Jade B labeling in hippocampus corresponded with clearly identifiable neurons in the CA1 or CA3 pyramidal cell layers or dentate granule cell layer. To more precisely determine the identity of the affected cells in the neocortex, double labeling with Neu-N, a neuron-specific antigen, was performed in conjunction with TUNEL staining. Approximately 75% of the TUNEL-positive cells in the neocortex were double-labeled with Neu-N (Fig. 4), indicating that neurons accounted for the majority of cell death in both neocortex and hippocampus.

Low-frequency glutamatergic synaptic transmission is normal in Tsc1^{GFAP}CKO mice

To determine whether the impaired glutamate homeostasis affects synaptic physiology in *Tsc1*^{GFAP}CKO mice, we assessed glutamatergic synaptic transmission in hippocampal slices. As we have previously documented that glutamate transporter function is impaired in astrocytes in the CA1 region of hippocampal slices from *Tsc1*^{GFAP}CKO mice (Wong et al., 2003), we examined glutamatergic excitatory postsynaptic currents (EPSCs) at the Schaffer collateral–CA1 pyramidal neuron synapse in hippocampal slices *in situ*. There were no significant differences in non-

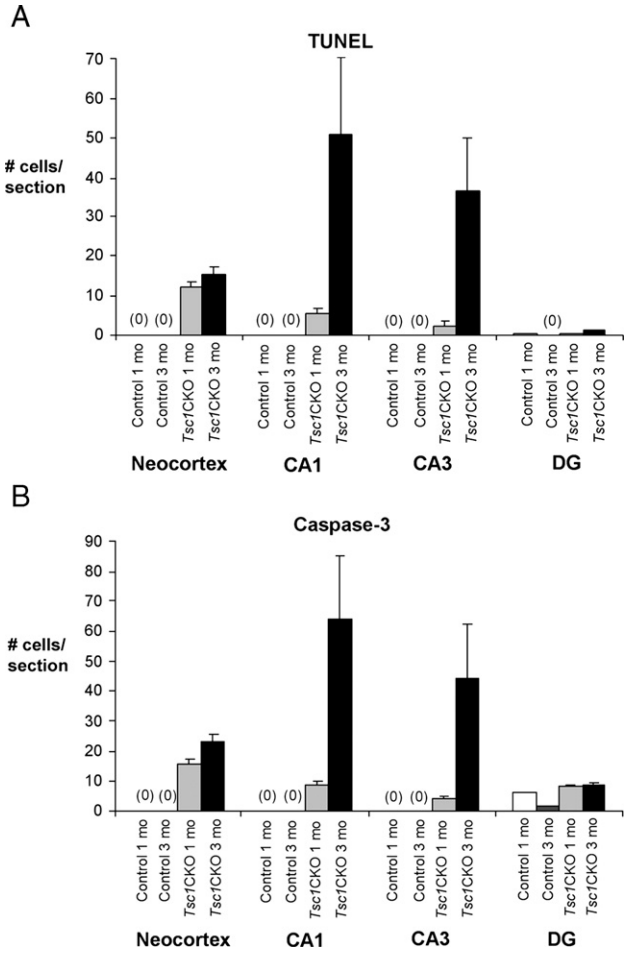

Fig. 3. Spatial and temporal distribution of TUNEL- and caspase-3-positive cells in *Tsc1*^{GFAP}CKO and control mice. Numbers of TUNEL- (A) and caspase-3- (B) positive cells in neocortical or hippocampal regions per section were counted in a blinded fashion in 1- and 3-month-old control and *Tsc1*^{GFAP}CKO mice ($n=3$ sections per mouse, 4–5 mice per group). There was a significant difference between control and *Tsc1*^{GFAP}CKO mice in TUNEL and caspase-3 staining in neocortex, CA1, and CA3 regions ($p<0.05$ by ANOVA for overall comparison between all 4 groups; $p<0.05$ for post-tests between control and *Tsc1*^{GFAP}CKO mice at both 1 and 3 months). Despite an apparent trend towards increased cell death between 1- and 3-month-old *Tsc1*^{GFAP}CKO mice in CA1 and CA3 regions of hippocampus, there were no statistically significant differences in TUNEL or caspase-3 staining between 1- and 3-month-old *Tsc1*^{GFAP}CKO mice.

NMDA or NMDA-mediated EPSCs in CA1 neurons activated at low frequency (0.1 Hz) from hippocampal slices obtained from 2- to 4-week-old control and *Tsc1*^{GFAP}CKO mice (Fig. 5; Table 1). In addition, there were no significant differences in the effect of the glutamate transporter antagonists, DHK or TBOA, on EPSCs in control vs. *Tsc1*^{GFAP}CKO hippocampal slices (data not shown). Since glutamate transporters exhibit significant temperature-sensitivity (Tong and Jahr, 1994), experiments were conducted at both room temperature and ~33 °C with similar results. Lastly, as inhibitory interneurons may be dependent upon astrocyte glutamate uptake and the subsequent shunting of glutamine for GABA synthesis (Patel et al., 2001), we also evaluated GABAergic IPSCs in the CA1 pyramidal neurons. There were no significant differences in GABAergic IPSCs between control and *Tsc1*^{GFAP}CKO hippocampal slices (Fig. 5; Table 1).

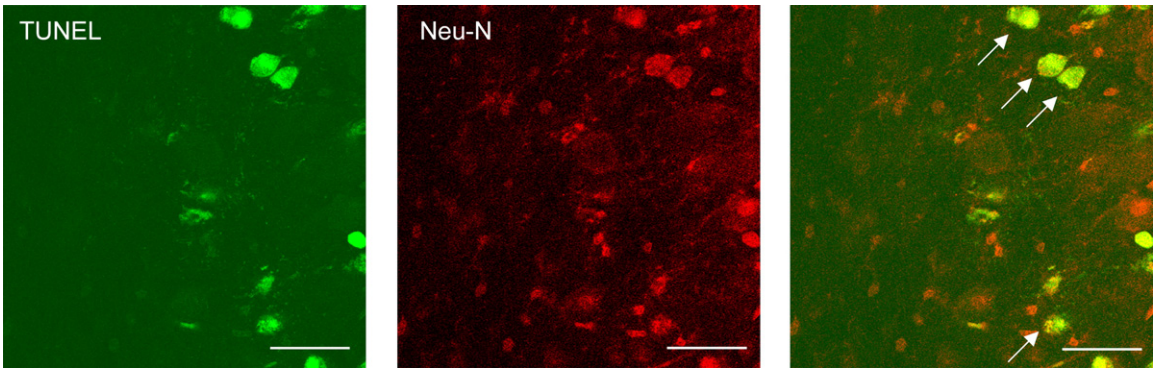

Fig. 4. The majority of TUNEL-positive cells in neocortex of *Tsc1*^{GFAP}CKO mice are neurons. Double labeling demonstrated that the majority of TUNEL-positive cells in neocortex of *Tsc1*^{GFAP}CKO mice were also positive for Neu-N, a neuronal marker. Examples of double-labeled cells marked by arrows. Calibration bars = 50 μm for all panels.

Hippocampal LTP is impaired in Tsc1^{GFAP}CKO mice due to elevated synaptic glutamate

While there were no significant abnormalities in glutamatergic synaptic transmission in *Tsc1*^{GFAP}CKO mice under conditions of low-frequency synaptic stimulation, we next sought to determine the effect of impaired astrocyte glutamate transport on long-term potentiation due to high-frequency synaptic stimulation. We considered this possibility based on the findings in *Glt1* knockout mice, which also exhibit normal glutamatergic synaptic transmission during low-frequency stimulation (Tanaka et al., 1997), but display impaired LTP due to excessive synaptic glutamate exposure (Katagiri et al., 2001). Stable, extracellular field EPSPs were activated in the stratum radiatum of CA1 region of hippocampal slices. Baseline field EPSPs activated by low-frequency synaptic stimulation (0.016 Hz) appeared to have a lower amplitude in *Tsc1*^{GFAP}CKO mice compared to control mice (Fig. 6A; 0.87 ± 0.40 mV measured at one-third maximal amplitude in *Tsc1*^{GFAP}CKO mice vs. 1.23 ± 0.40 in controls; $n = 6$ mice per group), but this difference was not statistically significant. However, LTP induced by tetanic stimulation (100 Hz) was significantly decreased in *Tsc1*^{GFAP}CKO mice compared to control mice (Figs. 6B, C; 105.6 ± 9.3% of baseline EPSP slope in *Tsc1*^{GFAP}CKO mice vs. 156.2 ± 10.3% in controls; $n = 6$ mice per group, $p < 0.05$). Furthermore, similar to *Glt-1* knockout mice (Katagiri et al., 2001), this impairment of LTP was partially reversed by application of a low concentration of D-APV (0.5 μM; to partially block NMDA receptors) during the tetanic stimulation in *Tsc1*^{GFAP}CKO mice (Figs. 6B, C; 137.9 ± 11.8% of baseline in the presence of D-APV vs. 105.6 ± 9.3% in the absence of D-APV; $n = 6$–8 mice per group, $p < 0.05$), suggesting that the impairment of LTP in *Tsc1*^{GFAP}CKO mice was due to excessive activation of NMDA receptors by glutamate.

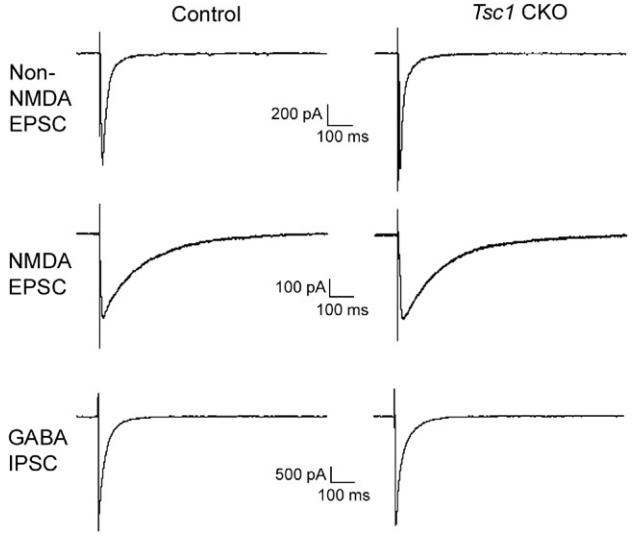

Fig. 5. Low-frequency glutamatergic synaptic transmission is normal in CA1 neurons in hippocampal slices from *Tsc1*^{GFAP}CKO mice. Representative traces show excitatory and inhibitory postsynaptic currents mediated by non-NMDA, NMDA and GABA receptors in CA1 neurons in response to low-frequency (0.1 Hz) stimulation of Schaffer collaterals in control and *Tsc1*^{GFAP}CKO hippocampal slices. See Table 1 for quantitative analysis.

Tsc1^{GFAP}CKO mice exhibit deficits in "hippocampal-dependent" conditioning/learning tasks

Given the impaired LTP and cell death observed in the hippocampus of *Tsc1*^{GFAP}CKO mice, we next tested the mice for

Table 1
Amplitude and decay kinetics of excitatory and inhibitory postsynaptic currents of CA1 neurons in hippocampal slices from control and *Tsc1*^{GFAP}CKO mice

	Control	*Tsc1*^{GFAP}CKO
Non-NMDA EPSC	$n = 12$	$n = 12$
I_{max}/C_m (pA/pF)	8.0 ± 1.5	8.4 ± 1.2
τ (ms)	12.6 ± 2.1	15.7 ± 2.2
NMDA EPSC	$n = 13$	$n = 11$
I_{max}/C_m (pA/pF)	3.6 ± 0.6	4.0 ± 1.2
τ (ms)	101.3 ± 7.0	118.9 ± 12.1
GABA IPSC	$n = 10$	$n = 12$
I_{max}/C_m (pA/pF)	17.8 ± 4.2	18.7 ± 5.7
τ (ms)	39.6 ± 5.6	42.3 ± 5.8

I_{max}/C_m – peak synaptic current normalized to membrane capacitance; τ – weighted time constant fitting the decay of the synaptic current with a two-exponential function. There was no significant difference in any parameter comparing control and *Tsc1*^{GFAP}CKO mice. Data shown are from experiments done at 33 °C.

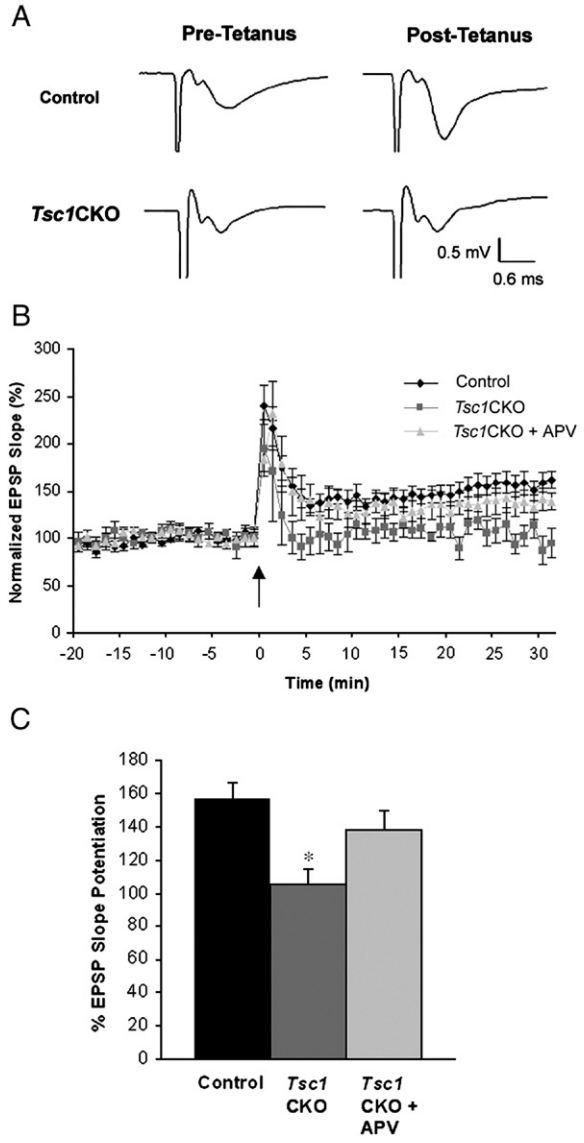

Fig. 6. Long-term potentiation induced by high-frequency synaptic stimulation is impaired in hippocampal slices from *Tsc1*^{GFAP}CKO mice. (A) Representative examples of field EPSPs in the CA1 region before and after tetanic (100 Hz) stimulation to the Schaffer collaterals to activate LTP. (B) Normalized initial EPSP slope from *Tsc1*^{GFAP}CKO mice demonstrate a significant decrease in LTP following the tetani (arrow) compared to control mice. Application of 0.5 μM D-APV during the period of tetanic stimulation (10 min before and after tetanic stimulation) partially reversed the decrease in LTP in *Tsc1*^{GFAP}CKO mice. (C) Average potentiation ratio (% of baseline field EPSP slope) with LTP in control slices, untreated *Tsc1*^{GFAP}CKO slices, and *Tsc1*^{GFAP}CKO slices treated with 0.5 μM D-APV was significantly reduced in untreated *Tsc1*^{GFAP}CKO slices (n=6–8 slices per group; *p<0.05 by ANOVA).

performance on two behavioral learning tasks that rely on intact hippocampal function (Silva et al., 1998; Maren and Holt, 2000): a Pavlovian-conditioned fear task and a spatial (place) learning/Morris water navigation task.

Conditioned fear

When first introduced into the conditioning chamber (Day 1), the *Tsc1*^{GFAP}CKO mice tended to freeze more often than controls (Fig. 7A) although an ANOVA of the freezing behavior over the 2-min baseline period did not yield any significant overall effects involving genotype. In contrast, analysis of the freezing data following the three tone(T)/shock(S) pairings showed that the control mice froze more often than the *Tsc1*^{GFAP}CKO mice, as documented by a significant main effect of genotype [F(1,16)=5.33, p=0.035]. Subsequent pairwise comparisons showed that the *Tsc1*^{GFAP}CKO mice froze much less often than controls after the second (p=0.024) and third T/S pairing (p=0.007; less than Bonferroni-corrected, p=0.017), suggesting that *Tsc1*^{GFAP}CKO mice may be impaired in short-term context conditioning. When re-introduced into the conditioning chamber 24 h after T/S training (Day 2), the *Tsc1*^{GFAP}CKO mice exhibited virtually no freezing behavior suggesting profound impairment in terms of contextual fear conditioning (Fig. 7B). In contrast, the control mice froze often during the first half of the test period indicating strong contextual fear conditioning. An ANOVA of the freezing data revealed a significant main effect of genotype [F(1,16)=7.87, p=0.013] and a significant Minute×Genotype interaction [F(7,112)=5.43, p=0.001]. Another striking aspect about the contextual fear data was that the control mice showed a gradual, steady decline in freezing over time after peaking at 2 min, thus demonstrating habituation (min 2 vs. min 8; p=0.001), whereas the *Tsc1*^{GFAP}CKO mice did not habituate but rather showed potentiation of freezing over most of the session (min 1 vs. min 7 (peak); p=0.025). Thus, control and *Tsc1*^{GFAP}CKO mice showed virtually opposite behavioral responses to the contextual cues that were paired with the shock.

To evaluate conditioning to the auditory cues (tone), the mice were placed into a new chamber (Day 3) containing different sets of visual, tactual, and olfactory cues 24 h after the contextual fear test, and both groups exhibited similar amounts of freezing over the 2-min baseline period (Fig. 7C). In contrast, the onset of the "tone" elicited much more freezing in control mice compared to the *Tsc1*^{GFAP}CKO mice (Fig. 7C), as evidenced by a significant Genotype×Minute interaction [F(7,98)=9.10, p<0.0005]. Subsequent pairwise comparisons showed that the control mice froze significantly more often than *Tsc1*^{GFAP}CKO mice during minute 1 (p<0.0005) and minute 2 (p=0.009). Similar to the contextual fear data, the control mice showed gradual but significant habituation of freezing over time (Block 1 vs. Block 8: p=0.006), while the *Tsc1*^{GFAP}CKO mice exhibited a significant potentiation of the freezing response across most of the test session (Block 1 vs. Block 7, peak freezing: p=0.044). The mice were also tested for their sensitivity to shock to determine if this may have contributed to the abnormal conditioning, but there were no differences between control and *Tsc1*^{GFAP}CKO mice in terms of the levels of shock that elicited flinching, running, vocalizing or jumping (Fig. 7D). One *Tsc1*^{GFAP}CKO mouse exhibited seizure-like behaviors during conditioned fear testing which appeared to produce long-term effects on its behavior and conditioning performance and therefore was eliminated from the dataset.

Morris water navigation

In the cued trials in the water maze, no differences were observed between *Tsc1*^{GFAP}CKO and control mice in escape path length (Fig. 7E) or latency (not shown), indicating that *Tsc1*^{GFAP}CKO mice had no deficits in non-associative functions (e.g., visual, sensorimotor, or motivational disturbances) that would affect their performance on subsequent place trials. In contrast, the *Tsc1*^{GFAP}CKO mice were significantly impaired

during acquisition in the place condition (Fig. 7F) relative to the controls. Specifically, an ANOVA of the path length data revealed a significant main effect of genotype [$F(1,7)=6.56$, $p=0.020$] showing that the controls had significantly shorter path lengths to the escape platform across the blocks of trials with differences between groups being greatest during the second ($p=0.004$) and eighth blocks ($p=0.049$) of trials. Also, control mice showed significant improvement between the first and last block of trials ($p=0.024$) suggesting that spatial learning had occurred while no such learning was observed in *Tsc1*^{GFAP}CKO mice. Differences between groups were even larger when escape latency was analyzed (data not shown); however, the latency data were confounded by the finding that *Tsc1*^{GFAP}CKO mice swam significantly slower than controls during the place trials (see below), thus making path length to the submerged platform the more appropriate dependent variable to assess acquisition performance during the place trials. An ANOVA of the swimming speed data resulted in a significant main effect of genotype [$F(1,17)=7.64$, $p=0.013$] indicating that the control mice swam significantly faster than the *Tsc1*^{GFAP}CKO mice across the blocks of trials (Fig.

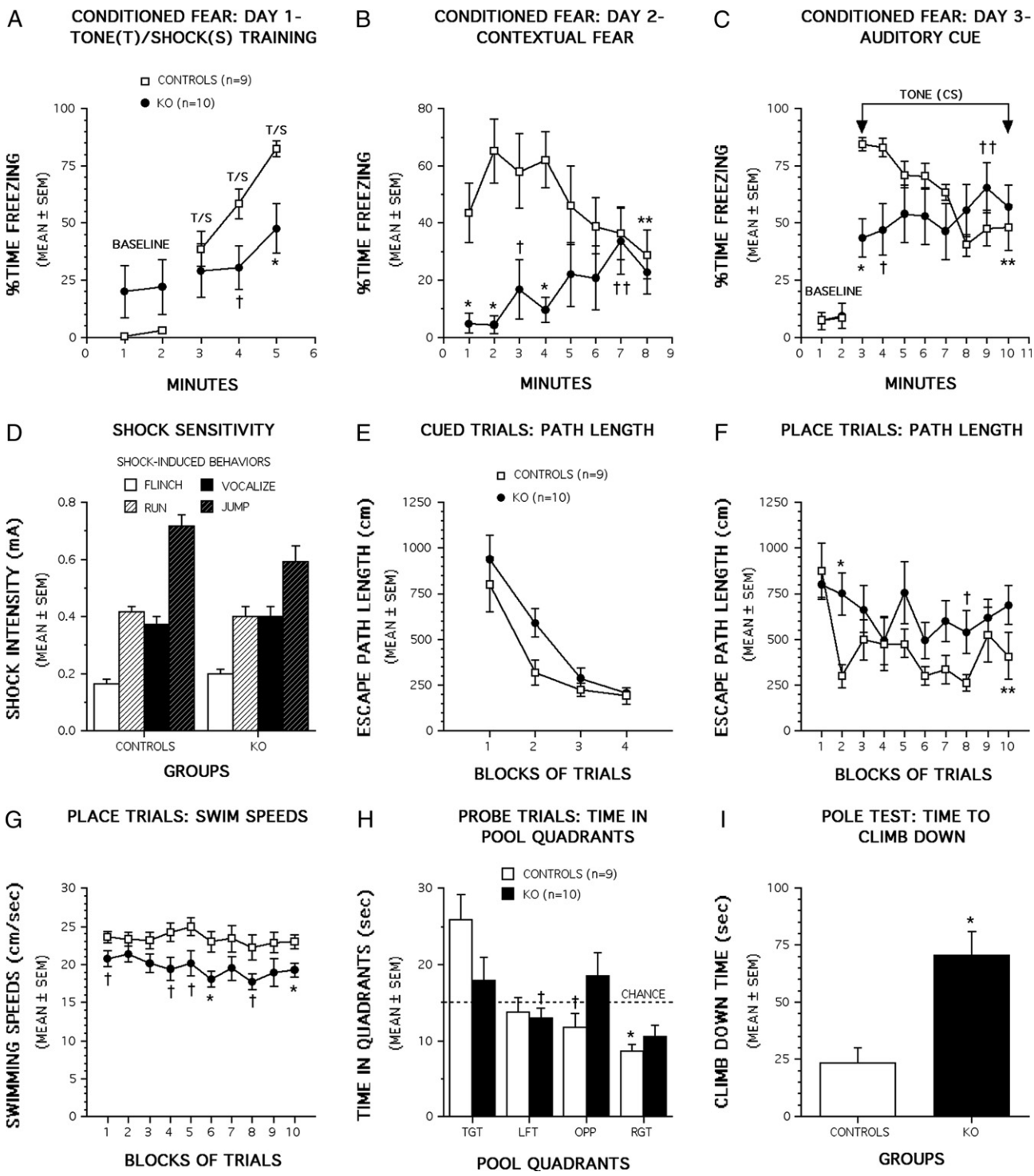

7G), with differences being greatest during the sixth and tenth blocks ($p<0.009$). With regard to the probe trial data, one-way ANOVAs conducted within each group on the times spent in the pool quadrants showed significant differences in quadrant times for controls [$F(3,24)=8.91$, $p=0.006$] but not *Tsc1*^{GFAP}CKO mice. Subsequent pairwise comparisons showed that control mice, but not *Tsc1*^{GFAP}CKO mice, exhibited spatial bias in spending more time in the quadrant that had contained the platform (target quadrant) compared to the left ($p=0.044$), opposite ($p=0.022$), and right ($p<0.0005$) quadrants (Fig. 7H), again indicating an impairment in spatial learning in the *Tsc1*^{GFAP}CKO mice.

Other relevant behavioral data

To provide important control data for aiding interpretation of the conditioning and learning results, as well as to characterize the behavioral phenotype of *Tsc1*^{GFAP}CKO mice in more detail, mice were evaluated on a battery of sensorimotor tests and on a 1-h locomotor activity measure. No significant differences were observed between the two groups of mice on the walking initiation, ledge, platform, 60° inclined screen, 90° inclined screen, or inverted screen tests from the sensorimotor battery when the mice were assessed during the early postweaning period (P25±1; data not shown). However, *Tsc1*^{GFAP}CKO mice (Fig. 7I) were significantly impaired on the pole test, which was originally developed to study bradykinesia associated with striatal dopamine depletion in mice. *Tsc1*^{GFAP}CKO mice took significantly longer to climb down the pole compared to controls ($t_{17}=3.69$, $p=0.002$), a finding that is consistent with the swimming speed data from the water maze testing. With regard to the activity data, no significant differences between groups were observed on any of the activity or emotionality variables when the mice were evaluated just before undergoing place training in the water maze (P32±1; data not shown). In summary, except for slow movement during a difficult task that requires complex coordination between the forelimbs and hindlimbs, the *Tsc1*^{GFAP}CKO mice were not impaired in a wide variety of motor/sensorimotor functions. These results and the lack of differences in the path length and latency data during the cued trials in the water maze suggest that the impaired acquisition performance of the *Tsc1*^{GFAP}CKO mice during the place trials and the contextual fear studies were not secondary to non-associative sources, but represent primary learning and conditioning deficits in these mice.

Discussion

The mechanisms underlying neuronal dysfunction in TSC are poorly understood. We have previously shown that *Tsc1*^{GFAP}CKO mice have impaired astrocyte glutamate transport, suggesting a potential role of disturbed glutamate homeostasis in TSC pathophysiology. In the present study, we report that extracellular glutamate is elevated in *Tsc1*^{GFAP}CKO mice *in vivo*. Furthermore, we show that *Tsc1*^{GFAP}CKO mice exhibit increased excitotoxic neuronal death and impaired synaptic plasticity, as well as associated behavioral deficits in hippocampal-dependent learning. Remarkably, the impairment in hippocampal synaptic plasticity is partially reversed by a glutamate antagonist at low dose, indicating that in addition to cell death, excessive synaptic glutamate directly causes this defect in synaptic function. These results are novel in indicating that abnormal glutamate homeostasis may contribute to mechanisms of neuronal dysfunction and cognitive deficits in TSC.

Given the dramatic reduction in astrocyte glutamate transport in *Tsc1*^{GFAP}CKO mice (Wong et al., 2003), it is not surprising that we observed elevated extracellular glutamate levels in the *Tsc1*^{GFAP}CKO mice. Previous studies indicate that astroglia glutamate transporters are responsible for the majority of glutamate transport and inactivation of these transporters leads to increased extracellular glutamate levels (Tanaka et al., 1997; Rothstein et al., 1996). While other confounding factors, such as seizures, might also contribute to elevated extracellular glutamate levels in *Tsc1*^{GFAP}CKO mice, the age used in the microdialysis studies likely precedes the age of onset of seizures in these mice (see below). Thus, we suggest that elevated glutamate levels most likely constitute a primary pathogenic factor promoting neuronal death and impaired synaptic function in *Tsc1*^{GFAP}CKO mice.

Significant neuronal death was observed in *Tsc1*^{GFAP}CKO mice in this study, potentially resulting from the elevated extracellular glutamate. Previous studies have shown that astrocytes protect neurons from glutamate-mediated excitotoxic cell death (Rosen-

Fig. 7. *Tsc1*^{GFAP}CKO mice exhibit deficits in contextual fear conditioning and spatial learning. (A) Although *Tsc1*^{GFAP}CKO mice tended to freeze more often than controls when the mice were first placed in the training chamber (baseline, Day 1), differences were not significant. However, control mice froze significantly ($p=0.035$) more often following the tone (T)/shock(S) pairings with significant (*) differences being observed following the third T/S pairing, suggesting that *Tsc1*^{GFAP}CKO mice may have had short-term context deficits. $^{\dagger}p=0.024$; $^{*}p=0.007$. (B) *Tsc1*^{GFAP}CKO mice showed profound deficits in contextual fear conditioning (Day 2) when tested 24 h after T/S training with differences being greatest during the first 4 min of the testing ($^{*}p<0.003$; $^{\dagger}p=0.024$). In addition, control mice showed habituation of the freezing response after peaking at 2 min (min 2 vs. min 8; $^{**}p=0.001$), while *Tsc1*^{GFAP}CKO showed a potentiation of freezing over most of the session [min 1 vs. min 7 (peak); $^{\dagger\dagger}p=0.025$]. (C) *Tsc1*^{GFAP}CKO and control mice showed similar levels of freezing when first introduced into the altered environment (baseline, Day 3) of the new chamber used to test auditory cue conditioning. However, control mice showed significantly greater levels of freezing following the onset of the tone compared to the *Tsc1*^{GFAP}CKO group ($^{*}p<0.0005$; $^{\dagger}p=0.009$). Again, control mice showed significant habituation of the freezing response (Block 1 vs. Block 8: $^{**}p=0.006$), while the *Tsc1*^{GFAP}CKO mice exhibited a significant potentiation of freezing across most of the test session [Block 1 vs. Block 7 (peak freezing: $^{\dagger\dagger}p=0.044$). (D) Control and *Tsc1*^{GFAP}CKO mice did not differ in the shock levels which elicited various behaviors (flinching, running, vocalizing, jumping) indicating that *Tsc1*^{GFAP}CKO mice did not have alterations in shock sensitivity which could account for differences in conditioning. (E) No differences between groups were observed in terms of path length during cued trials in the water maze. (F) However, *Tsc1*^{GFAP}CKO showed a significant deficit in spatial learning acquisition during place trials in the water maze where controls had significantly shorter path lengths to the escape platform across the blocks of trials with differences being greatest during the second ($^{*}p=0.004$) and eighth blocks ($^{\dagger}p=0.049$) of trials. Also, control mice showed significant improvement between the first and last block of trials ($^{**}p=0.024$) suggesting learning had occurred while *Tsc1*^{GFAP}CKO mice showed no such improvement. (G) *Tsc1*^{GFAP}CKO swam significantly slower than controls during the place trials, thus making path length to the submerged platform a more appropriate dependent variable than latency to assess acquisition performance during the place trials. Differences between groups were greatest during the sixth and tenth blocks ($^{*}p<0.009$; $^{\dagger}p<0.029$). (H) Retention data collected during the probe trial suggested that control mice, but not *Tsc1*^{GFAP}CKO mice, displayed spatial memory by spending more time in the target quadrant, which had contained the submerged platform, than in the quadrants to the left ($^{\dagger}p=0.044$), right ($^{*}p=0.001$), or opposite ($^{\dagger}p=0.022$) of the target quadrant. (I) The pole test was the only measure out of all activity and sensorimotor variables where significant differences were found between *Tsc1*^{GFAP}CKO and control mice. Specifically, *Tsc1*^{GFAP}CKO mice were found to take significantly longer to climb down the pole ($p=0.002$).

berg and Aisenman, 1989; Ye and Sontheimer, 1998) and inactivation of glutamate transporters induces neuronal death *in vivo* (Rothstein et al., 1996; Tanaka et al., 1997). While impaired astrocyte glutamate transport represents a rational mechanism for the observed neuronal injury in *Tsc1*^{GFAP}CKO mice, potential confounding effects of other factors, in particular seizures, on cell death again need to be considered, as seizures by themselves can cause neuronal death. To control for the effect of seizures, we assayed cell death at two time points, corresponding to times before and after the usual onset of seizures, based on previous video-EEG studies (Uhlmann et al., 2002; Erbayat-Altay et al., 2007). *Tsc1*^{GFAP}CKO mice typically exhibit onset of epilepsy between 1 and 2 months of age with infrequent seizures. By 2 to 3 months of age, seizures progressively worsen in frequency and severity, culminating in death by 3 to 4 months of age. In the present study, we observed a trend towards increased neuronal death in the hippocampus of *Tsc1*^{GFAP}CKO mice at 3 months of age compared to 1 month, suggesting a possible additional effect of seizures on neuronal death. However, the presence of neuronal death in both neocortex and hippocampus at 1 month of age and the lack of definite progression in cell death with age, especially in neocortex, indicates that neuronal death is likely an independent event preceding seizures in *Tsc1*^{GFAP}CKO mice and may be related to elevated extracellular glutamate levels from impaired astrocyte glutamate transport. Thus, neuronal death triggered by excessive glutamate may contribute to the development of epileptogenesis and other neurological deficits in these mice. Of clinical relevance, markers of cell death have also been found in cortical tubers from patients with TSC (Maldonado et al., 2003).

Impaired glutamate transport and elevated extracellular glutamate levels could also have direct effects on synaptic function. However, glutamatergic synaptic transmission was normal in hippocampal slices from *Tsc1*^{GFAP}CKO mice under conditions of low-frequency stimulation. Although some studies have reported a modest effect of glutamate transporter antagonists on excitatory postsynaptic currents (Mennerick and Zorumski, 1994; Tong and Jahr, 1994), others have found no effect (Isaacson and Nicoll, 1993; Sarantis et al., 1993; Tanaka et al., 1997), indicating that glutamate transport has minimal contribution to rapid, post-synaptic glutamatergic responses during low-frequency synaptic transmission. In contrast, LTP induced by tetanic stimuli was impaired in *Tsc1*^{GFAP}CKO mice, suggesting that abnormal glutamate transport and elevated extracellular glutamate are more likely to impact synaptic function during maximal glutamate release, such as with high-frequency tetanic synaptic signalling. The reduction in LTP could be related to the neuronal death seen in hippocampus in *Tsc1*^{GFAP}CKO mice, as well as other circuit abnormalities. Interestingly, however, this impairment in LTP was reversed by the presence of low concentrations of a NMDA antagonist, suggesting that excessive synaptic glutamate, at least in part, can directly account for abnormal synaptic plasticity. Analogously, *Glt-1* knockout mice also exhibit normal low-frequency glutamate synaptic transmission but impaired LTP that is reversed with low concentrations of APV (Katagiri et al., 2001; Tanaka et al., 1997). Other studies suggest that excessive NMDA receptor activation may also impair LTP in normal rodent hippocampus (Bashir and Collingridge, 1992; Coan et al., 1989). Collectively, our findings suggest that elevated extracellular glutamate in *Tsc1*^{GFAP}CKO mice may cause pathologically excessive activation of NMDA receptors during high-frequency synaptic stimulation, which may result in impaired LTP induction. Consistent with a recent report of abnormal synaptic plasticity in the Eker rat model of TSC (Von der Brelie et al., 2006), impaired LTP in *Tsc1*^{GFAP}CKO mice could provide a mechanistic explanation for cognitive deficits commonly seen in TSC.

In support of this idea, our behavioral studies demonstrate significant deficits in two hippocampal-dependent conditioning/learning paradigms. First, in a Pavlovian-conditioned fear task, *Tsc1*^{GFAP}CKO mice showed virtually no evidence of contextual fear conditioning, despite an intact sensitivity to shock compared to controls. Moreover, the responses of *Tsc1*^{GFAP}CKO mice during tone–shock training suggest that short-term memory deficits pertaining to aversive stimuli may have also contributed to their contextual fear conditioning impairments, a possibility that should be evaluated in future studies. Second, the water maze data suggest that compromised cognitive functions of *Tsc1*^{GFAP}CKO mice extend to spatial learning and memory, although the magnitude of this impairment was not as profound. Differences between the control and *Tsc1*^{GFAP}CKO mice in spatial learning may have been even greater with an extended testing period, since controls would have likely continued to improve with additional testing relative to the *Tsc1*^{GFAP}CKO mice who showed no evidence of learning by the fifth block of trials. Unfortunately, our design was limited by our need to obtain other important behavioral data (e.g., conditioned fear, sensorimotor battery) within a constrained time frame, to minimize possible confounding effects of seizures.

Although other factors could have confounded interpretation of the behavioral results, the bulk of the present data indicate that *Tsc1*^{GFAP}CKO mice have primary cognitive deficits in hippocampal-dependent tasks. The lack of significant performance differences between groups on all activity measures, on 6 of 7 sensorimotor tests, in shock sensitivity, and during the cued water maze trials indicates that the impaired conditioning and learning performance of *Tsc1*^{GFAP}CKO mice was not secondary to compromised non-associative functions. The one deficit found in *Tsc1*^{GFAP}CKO mice relating to complex co-ordination functions likely did not have a significant impact on conditioning/learning performance, given the normal performance of *Tsc1*^{GFAP}CKO mice on all activity measures and during the cued trials. As discussed for the other experiments, the presence of seizures could also affect certain behavioral indices. However, the effect of seizures was likely minimal, since most of the behavioral testing occurred at an age that was likely prior to seizure onset (see above) and we were careful to monitor for seizure activity and minimize direct confounding effects on behavior. Future behavioral studies are warranted to determine if there are other significant functional impairments in these mice.

We appreciate that additional studies are needed to more definitively prove a causal link between impaired astrocyte-regulated glutamate homeostasis and the associated neurological phenotype in *Tsc1*^{GFAP}CKO mice. Although multiple lines of evidence indicate that astrocytes play a key role in the pathophysiology of *Tsc1*^{GFAP}CKO mice, it is possible that *Tsc1* inactivation in GFAP-positive neuroglial progenitor cells during early cortical development could lead to primary neuronal defects, which could also contribute to abnormal glutamatergic synaptic physiology and impaired learning in these mice. Future experiments in our laboratory will test the effect of pharmacological or genetic manipulations that upregulate astrocyte glutamate transporters on reversing the glutamate-related abnormalities observed in the present study (Ganel et al., 2006; Rothstein et al., 2005), thus potentially providing mechanistic proof for the importance of

astrocytic regulation of glutamate homeostasis in this model. Of clinical relevance, the findings of impaired glutamate homeostasis and associated abnormalities in synaptic plasticity and neuronal death in *Tsc1*^{GFAP}CKO mice represent rational mechanisms that may contribute to cognitive deficits and epileptogenesis in TSC and suggest the possibility of novel therapeutic approaches for TSC directed specifically at astrocyte glutamate transport, or glutamate homeostasis in general.

Acknowledgments

We thank Nicholas Rensing and Sara Conyers for technical support. This work was supported by grants from the National Institutes of Health (K02NS045583 and R01NS056872, MW; DA07261, JRC; Neuroscience Blueprint Core Grant NS057105), Tuberous Sclerosis Alliance (MW), and U.S. Army Medical Research and Materiel Command grant (DAMD17-03-1-0073, DHG).

References

Bashir, Z.I., Collingridge, G.L., 1992. NMDA receptor-dependent transient homo- and heterosynaptic depression in picrotoxin-treated hippocampal slices. Eur. J. Neurosci. 4, 485–490.

Biebl, M., Cooper, C.M., Winkler, J., Kuhn, H.G., 2000. Analysis of neurogenesis and programmed cell death reveals a self-renewing capacity in the adult rat brain. Neurosci. Lett. 291, 17–20.

Cirrito, J.R., May, P.C., O'Dell, M.A., Taylor, J.W., Parsadanian, M., Cramer, J.W., Audia, J.E., Nissen, J.S., Bales, K.R., Paul, S.M., DeMattos, R.B., Holtzman, D.M., 2003. In vivo assessment of brain interstitial fluid with microdialysis reveals plaque-associated changes in amyloid-β metabolism and half-life. J. Neurosci. 23, 8844–8853.

Cirrito, J.R., Yamada, K.A., Finn, M.B., Sloviter, R.S., Bales, K.R., May, P.C., Schoepp, D.D., Paul, S.M., Mennerick, S., Holtzman, D.M., 2005. Synaptic activity regulates interstitial fluid amyloid-β levels in vivo. Neuron 48, 913–922.

Coan, E.J., Irving, A.J., Collingridge, G.L., 1989. Low-frequency activation of the NMDA receptor system can prevent the induction of LTP. Neurosci. Lett. 105, 205–210.

Crino, P.B., Nathanson, K.L., Henske, E.P., 2006. The tuberous sclerosis complex. N. Engl. J. Med. 355, 1345–1346.

Doherty, C., Goh, S., Young Poissant, T., Erdaq, N., Thiele, E.A., 2005. Prognostic significance of tuber count and location in tuberous sclerosis complex. J. Child Neurol. 20, 837–841.

Erbayat-Altay, E., Zeng, L.H., Xu, L., Gutmann, D., Wong, M., 2007. The natural history and treatment of epilepsy in a murine model of tuberous sclerosis. Epilepsia 48, 1470–1476.

Ess, K.C., Uhlmann, E.J., Li, W., Li, H., DeClue, J.E., Crino, P.B., Gutmann, D.H., 2004. Expression profiling in tuberous sclerosis complex (TSC) knockout mouse astrocytes to characterize human TSC brain pathology. GLIA 46, 28–40.

Ganel, R., Ho, T., Maragakis, N.J., Jackson, M., Steiner, J.P., Rothstein, J.D., 2006. Selective up-regulation of the glial Na^+-dependent glutamate transporter GLT1 by a neuroimmunophilin ligand results in neuroprotection. Neurobiol. Dis. 21, 556–567.

Goodman, M., Lamm, S.H., Engel, A., Shepherd, C.W., Houser, O.W., Gomez, M.R., 1997. Cortical tuber count: a biomarker indicating neurologic severity of tuberous sclerosis complex. J. Child Neurol. 12, 85–90.

Gutmann, D.H., Zhang, Y., Hasbani, M.J., Goldberg, M.P., Plank, T.L., Henske, E.P., 2000. Expression of the tuberous sclerosis complex (TSC) gene products, *hamartin* and *tuberin*, in central nervous system tissues. Acta Neuropathol. 99, 223–230.

Isaacson, J.S., Nicoll, R.A., 1993. The uptake inhibitor L-*trans*-PDC enhances responses to glutamate but fails to alter the kinetics of excitatory synaptic currents in the hippocampus. J. Neurophys. 70, 2187–2191.

Katagiri, H., Tanaka, K., Manabe, T., 2001. Requirement of appropriate glutamate concentrations in the synaptic cleft for hippocampal LTP induction. Eur. J. Neurosci. 14, 547–553.

Khuchua, Z., Wozniak, D.F., Bardgett, M.E., Yue, Z., McDonald, M., Boero, J., Hartman, R.E., Sims, H., Strauss, A.W., 2003. Deletion of the N-terminus of murine *map2* by gene targeting disrupts hippocampal CA1 neuron architecture and alters contextual memory. Neuroscience 119, 101–111.

Kwiatkowski, D.J., 2003. Tuberous sclerosis: from tubers to mTOR. Ann. Hum. Genet. 67, 87–96.

Maldonado, M., Baybis, M., Newman, D., Kolson, D.L., Chen, W., McKhann, G., Gutmann, D.H., Crino, P.B., 2003. Expression of ICAM-1, TNF-alpha, NF kappa B, and MAP kinase in tubers of the tuberous sclerosis complex. Neurobiol. Dis. 14, 279–290.

Maren, S., Holt, W., 2000. The hippocampus and contextual memory retrieval in Pavlovian conditioning. Behav. Brain Res. 110, 97–108.

Menacherry, S., Hubert, W., Justice Jr., J.B., 1992. In vivo calibration of microdialysis probes for exogenous compounds. Anal. Chem. 64, 577–583.

Mennerick, S., Zorumski, C.F., 1994. Glial contributions to excitatory neurotransmission in cultured hippocampal cells. Nature 368, 59–62.

Patel, A.B., Rothman, D.L., Cline, G.W., Behar, K.L., 2001. Glutamine is the major precursor for GABA synthesis in rat neocortex in vivo following acute GABA-transaminase inhibition. Brain Res. 919, 207–220.

Rosenberg, P.A., Aisenman, E., 1989. Hundred-fold increase in neuronal vulnerability to glutamate toxicity in astrocyte-poor cultures of rat cerebral cortex. Neurosci. Lett. 103, 162–168.

Rothstein, J.D., Dykes-Hoberg, M., Pardo, C.A., Bristol, L.A., Jin, L., Kunci, R.W., Kanai, Y., Hediger, M.A., Wang, Y., Schielke, J.P., Welty, D.F., 1996. Knockout of glutamate transporters reveals a major role for astroglial transport in excitotoxicity and clearance of glutamate. Neuron 16, 675–686.

Rothstein, J.D., Patel, S., Regan, M.R., Haenggeli, C., Huang, Y.H., Bergles, D.E., Jin, L., Hoberg, M.D., Vidensky, S., Chung, D.S., Toan, S.V., Bruijn, L.I., Su, Z.Z., Gupta, P., Fisher, P.B., 2005. Beta-lactam antibiotics offer neuroprotection by increasing glutamate transporter expression. Nature 43, 73–77.

Sarantis, M., Ballerini, L., Miller, B., Silver, R.A., Edwards, M., Attwell, D., 1993. Glutamate uptake from the synaptic cleft does not shape the decay of the non-NMDA component of the synaptic cleft. Neuron 11, 541–549.

Schmued, L.C., Hopkins, K.J., 2000. Fluoro-Jade B: a high affinity fluorescent marker for the localization of neuronal degeneration. Brain Res. 874, 123–130.

Silva, A.J., Giese, K.P., Federov, N.B., Frankland, P.W., Kogan, J.H., 1998. Molecular, cellular, and neuroanatomical substrates of place learning. Neurobiol. Learn. Mem. 70, 44–61.

Sparagana, S.P., Roach, E.S., 2000. Tuberous sclerosis complex. Curr. Opin. Neurol. 13, 115–119.

Tanaka, K., Watase, K., Manabe, T., Yamada, K., Watanabe, M., Takahashi, K., Iwama, H., Nishikawa, T., Ichihara, N., Kikuchi, T., Okuyama, S., Kawashima, N., Hori, S., Takimoto, M., Wada, K., 1997. Epilepsy and exacerbation of brain injury in mice lacking the glutamate transporter GLT-1. Science 276, 1699–1702.

Tong, G., Jahr, C.E., 1994. Block of glutamate transporters potentiates postsynaptic excitation. Neuron 13, 1195–1203.

Uhlmann, E.J., Wong, M., Baldwin, R.L., Bajenaru, M.L., Onda, H., Kwiatkowski, D.J., Yamada, K., Gutmann, D.H., 2002. Astrocyte-specific TSC1 conditional knockout mice exhibit abnormal neuronal organization and seizures. Ann. Neurol. 52, 285–296.

Von der Brelie, C., Waltereit, R., Zhang, L., Beck, H., Kirschstein, T., 2006. Impaired synaptic plasticity in a rat model of tuberous sclerosis. Eur. J. Neurosci. 23, 686–692.

Watanabe, T., Morimoto, K., Hirao, T., Suwaki, H., Watase, K., Tanaka, K., 1999. Amygdala-kindled and pentylenetetrazole-induced seizures in glutamate transporter GLAST-deficient mice. Brain Res. 845, 92–96.

Wong, M., Ess, K.E., Uhlmann, E.J., Jansen, L.A., Li, W., Crino, P.B., Mennerick, S., Yamada, K.A., Gutmann, D.H., 2003. Impaired astrocyte glutamate transport in a mouse epilepsy model of tuberous sclerosis complex. Ann. Neurol. 54, 251–256.

Wozniak, D., Hartman, R.E., Boyle, M.P., Vogt, S.K., Brooks, A.R., Tenkova, T., Young, C., Olney, J.W., Muglia, L.J., 2004. Apoptotic neurodegeneration induced by ethanol in neonatal mice is associated with profound learning/memory deficits in juveniles followed by progressive functional recovery in adults. Neurobiol. Dis. 17, 403–414.

Ye, Z.C., Sontheimer, H., 1998. Astrocytes protect neurons from neurotoxic injury by serum glutamate. Glia 22, 237–248.